



University of HUDDERSFIELD

University of Huddersfield Repository

Cox, Nicola M, Harding, Lindsay P., Jones, Jennifer E., Pope, Simon JA, Rice, Craig R. and Adams, Harry

Probing solution behaviour of metallocupramolecular complexes using pyrene fluorescence

Original Citation

Cox, Nicola M, Harding, Lindsay P., Jones, Jennifer E., Pope, Simon JA, Rice, Craig R. and Adams, Harry (2012) Probing solution behaviour of metallocupramolecular complexes using pyrene fluorescence. *Dalton Transactions*, 41 (5). pp. 1568-1573. ISSN 14779226

This version is available at <http://eprints.hud.ac.uk/id/eprint/13204/>

The University Repository is a digital collection of the research output of the University, available on Open Access. Copyright and Moral Rights for the items on this site are retained by the individual author and/or other copyright owners. Users may access full items free of charge; copies of full text items generally can be reproduced, displayed or performed and given to third parties in any format or medium for personal research or study, educational or not-for-profit purposes without prior permission or charge, provided:

- The authors, title and full bibliographic details is credited in any copy;
- A hyperlink and/or URL is included for the original metadata page; and
- The content is not changed in any way.

For more information, including our policy and submission procedure, please contact the Repository Team at: E.mailbox@hud.ac.uk.

<http://eprints.hud.ac.uk/>

Probing solution behaviour of metallosupramolecular complexes using pyrene fluorescence

Nicola M. Cox,^a Lindsay P. Harding,^{*a} Jennifer E. Jones,^b Simon J. A. Pope,^b Craig R. Rice^a and Harry Adams^c

Abstract

A new method for assessing the topology of metallosupramolecular assemblies using pyrene-appended ligands is reported. Two potentially tetradentate ligands containing one (L^1) and two (L^2) terminal pyrene moieties were synthesised and their complexes with Cu^+ and Cd^{2+} were characterised. Photophysical measurements demonstrate that in $[Cu_2(L^1)_2]^{2+}$, $[CdL^1]^{2+}$ and $[Cu_2(L^2)_2]^{2+}$ the emission spectra are dominated by monomeric emission but in the cadmium complex of L^2 (where the pyrene units are in close proximity) a quenching of the luminescence coupled with weak emission at 540 nm is indicative of excimer formation.

Introduction

Formation of helicate complexes from self-assembly of polydentate ligands with metal ions has received much attention in recent years.¹ Control of these systems can be achieved by careful design of the binding domains within the ligand strand and selection of metal ions with a suitable coordination preference. For example, if a ligand contains four donor atoms it can act as a tetradentate donor coordinating octahedral metal ions in the equatorial positions giving a simple mononuclear complex $[ML]^{n+}$. However, upon reaction with a metal ion that prefers a tetrahedral coordination environment then the ligand will partition into two bidentate domains, each of which will coordinate a *different* metal ion. Coordination of an additional ligand results in a dinuclear double helicate of the formula $[M_2L_2]^{n+}$. The archetypal example of this behaviour is reaction of quaterpyridine with either Zn^{2+} or Cu^+ .^{2,3} With the dicationic metal, which prefers octahedral coordination, a simple mononuclear complex is formed with the zinc ion coordinated in the equatorial positions by all four *N*-donor atoms. With Cu^+ the ligand partitions into two bidentate domains each of which coordinates a different metal ion resulting in the self-assembly of a helicate system.

Generally, characterisation requires the use of single-crystal X-ray diffraction which gives valuable information on the self-assembly but analysis of crystals may only represent a species which is thermodynamically favoured in the solid state and may not reflect the composition of the bulk solution. NMR gives information on the symmetry of complexes but sophisticated experiments are required to get information on the topology of assemblies (e.g. from hydrodynamic radii, proximity of ligand strands). Mass spectrometry provides the stoichiometry of such species *via* their molecular masses but no information on how the ligands are arranged.

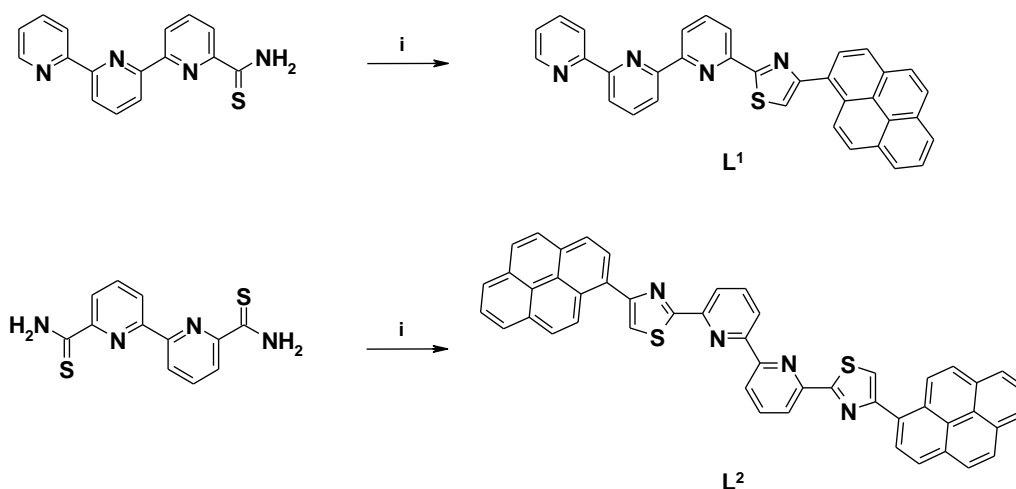
This paper describes a new technique for simple elucidation of solution behaviour of pyridyl-thiazole complexes appended with pyrene “tags”. Pyrene is a useful lumophore as the emission profile can give insight into the arrangement of these aromatic species in solution. Isolated pyrene units luminesce between 360–440 nm however close interaction between pyrene units results in energy transfer between these species (excimer luminescence) and the resultant emission is quenched and at lower energy (~ 500 nm). This approach has been used in biological applications including investigation of protein unfolding,⁴ detection of specific mRNA and DNA sequences⁵ and determination of conformational changes induced in *myo*-inositol 1,2,3-triphosphate upon binding Fe³⁺ ions.⁶ In this work, a phosphate sugar was appended with two pyrene groups which, when the sugar was in its preferred penta-equatorial conformation, were far apart. On binding Fe³⁺ ions, the sugar adopted the less energetically favoured penta-axial conformation to accommodate the metal ion and the two pyrenes became proximate; an intramolecular excimer species was formed. This conformational change was monitored using the pyrene luminescence emission; the luminescence spectrum of the free (unbound) pyrene-appended sugar showed a large, high energy band at 386 nm from monomeric pyrene whereas on binding Fe³⁺ an overall quenching of the luminescence was observed along with the appearance of a broad emission band at 510 nm, both of which phenomena are characteristic of excimer formation.

There are substantially fewer examples of synthetic pyrene-appended systems; the majority of these are used as sensors with conformational changes induced on binding the target analyte causing either increased or decreased excimer emission from the pyrene groups. Examples of such systems include sensors for ATP,⁷ heparin,⁸ nucleotides⁹ and transition metal ions.¹⁰ Pyrene-appended complexes have also found application in magnetic materials,¹¹ in the study of electron transfer within supramolecular complexes¹² and as building blocks for preparation of luminescent polymers.¹³

Results and discussion

Ligand synthesis

Both ligands were prepared by reaction of their corresponding thioamides (2,2':6'2''-terpyridine-6-thioamide for **L**¹ and 2,2'-bipyridine-6,6'-dithioamide for **L**²) with 1-(bromoacetyl)pyrene in ethanol in an analogous manner to related ligands reported previously (Scheme 1).¹⁴



Scheme 1 Synthesis of ligands **L¹** and **L²**: (i) 1-(bromoacetyl)pyrene, ethanol, reflux

Coordination chemistry

Reaction of **L¹** with **Cu(MeCN)₄PF₆**

Reaction of **L¹** with one equivalent of **Cu(MeCN)₄PF₆** in **MeNO₂** gave a red solution from which slow diffusion of ethyl acetate afforded red crystals. Solution state analyses indicated formation of the dinuclear double helicate species **[Cu₂(L¹)₂]²⁺**; analysis by electrospray ionisation mass spectrometry (ESI-MS) showed an ion at *m/z* 1305.1 corresponding to **{[Cu₂(L¹)₂](PF₆)⁺**. Single crystal X-ray analysis confirmed formation of **[Cu₂(L¹)₂]²⁺** and showed that the ligand partitions into two bidentate *N*-donor domains each of which coordinates a different metal ion (Fig. 1a,b).

Each copper ion is coordinated by two bidentate domains, one from each ligand. The Cu(I) centre adopts a distorted tetrahedral geometry with Cu–N distances ranging from 1.986(9) to 2.104(7) Å. As this is an asymmetric ligand it can be considered as having both a head and a tail. It is feasible that both head-to-tail and head-to-head isomers are formed; however, in the solid state only the head-totail isomer is observed which can be rationalised by consideration of the steric interactions within the complex. The intramolecular pyrene–pyrene separation is relatively large with an interstrand centroid···centroid distance of 11.138 Å. The extended molecular packing is shown in Fig. 1c; each of the pyrene units aligns in an edge-to-face manner with the average of the four shortest intermolecular centroid···centroid separations at 6.591 Å. The ¹H NMR spectrum (CD₃CN) showed the presence of major and minor components. The peaks were largely overlapping since up to 40 aromatic signals could be expected for the complex (if a mixture of the unsymmetrical head-to-tail and the symmetrical head-to-head isomers were formed in solution). However, the spectrum is consistent with formation of the **[Cu₂(L¹)₂]²⁺** complex.

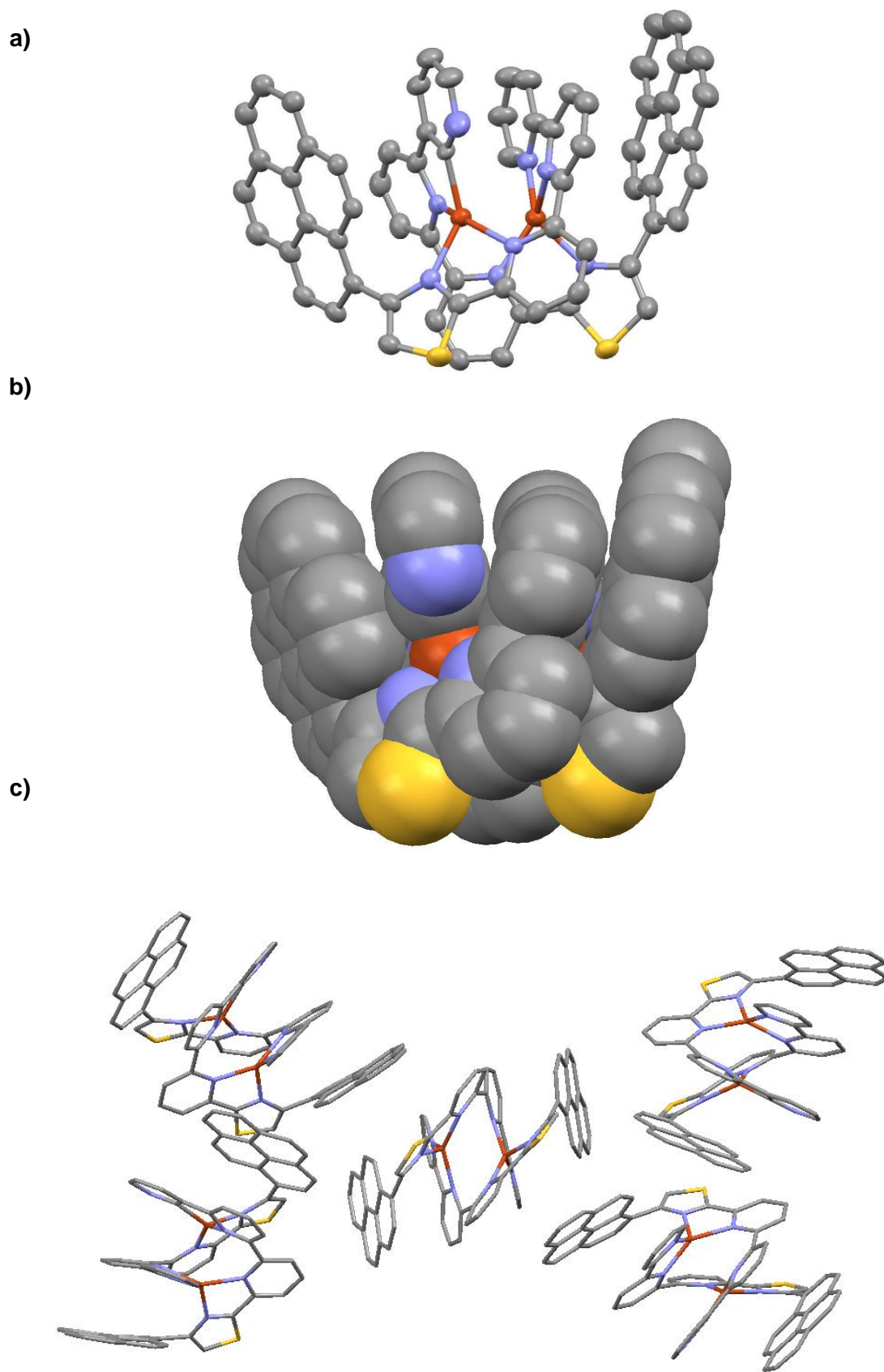


Fig.1 The single crystal structure of $[\text{Cu}_2\text{L}^1_2]^{2+}$: (a) as a displacement ellipsoid plot drawn at the 50% probability level; (b) as a space-filling model; (c) showing the molecular packing in the unit cell (counter ions omitted for clarity)

Reaction of L^1 with $Cd(ClO_4)_2 \cdot 6H_2O$

Reaction of L^1 with $Cd(ClO_4)_2 \cdot 6H_2O$ in nitromethane gave a yellow solution from which orange crystals were formed on slow diffusion of diethyl ether but these were not of sufficient quality for X-ray analysis. The 1H NMR spectrum (CD_3NO_2) shows aromatic signals from 20 protons which is consistent with formation of the mononuclear species $[Cd(L^1)]^{2+}$ in an analogous manner to the disubstituted ligand L^2 (see later); ESI-MS analysis showed an ion at m/z 729.0 corresponding to $\{[Cd(L^1)](ClO_4)\}^+$. The ligand is expected to act as a simple tetradentate *N*-donor with three pyridyl nitrogen atoms and one thiazole nitrogen atom coordinating all four equatorial positions of the metal centre in a similar way to that observed in the L^2 complex (see later).

Reaction of L^2 with $Cd(ClO_4)_2 \cdot 6H_2O$

Reaction of L^2 with one equivalent of $Cd(ClO_4)_2 \cdot 6H_2O$ in nitromethane gave a yellow solution from which orange crystals were deposited upon slow diffusion of ethyl acetate. An ion was observed in the ESI-MS at m/z 935.0 corresponding to the mononuclear species $\{[Cd(L^2)](ClO_4)\}^+$; the 1H NMR spectrum of the complex (CD_3NO_2) showed 13 aromatic signals which is also consistent with formation of $[Cd(L^2)]^{2+}$. Single crystal X-ray analysis confirmed the formation of the mononuclear species; in the solid state, the ligand acts as a tetradentate donor with all four nitrogen atoms coordinating the equatorial positions of the metal ion (Cd–N distances 2.276(2)–2.340(2) Å). The cadmium ion is further coordinated by two perchlorate ions (Cd–O distances 2.402(2)–2.418(2) Å) resulting in a six-coordinate metal centre (Fig. 2a,b). The two pyrene moieties are in close proximity with a centroid...centroid distance of 3.783 Å. The intermolecular pyrene–pyrene distances are quite long (shortest centroid–centroid distance 9.915 Å) and the pyrene units p-stack with the planar tetradentate pyridyl–thiazole domains (Fig. 2c). The shortest centroid...centroid distance is 4.824 Å which is significantly longer than the intramolecular pyrene–pyrene separation (3.783 Å).

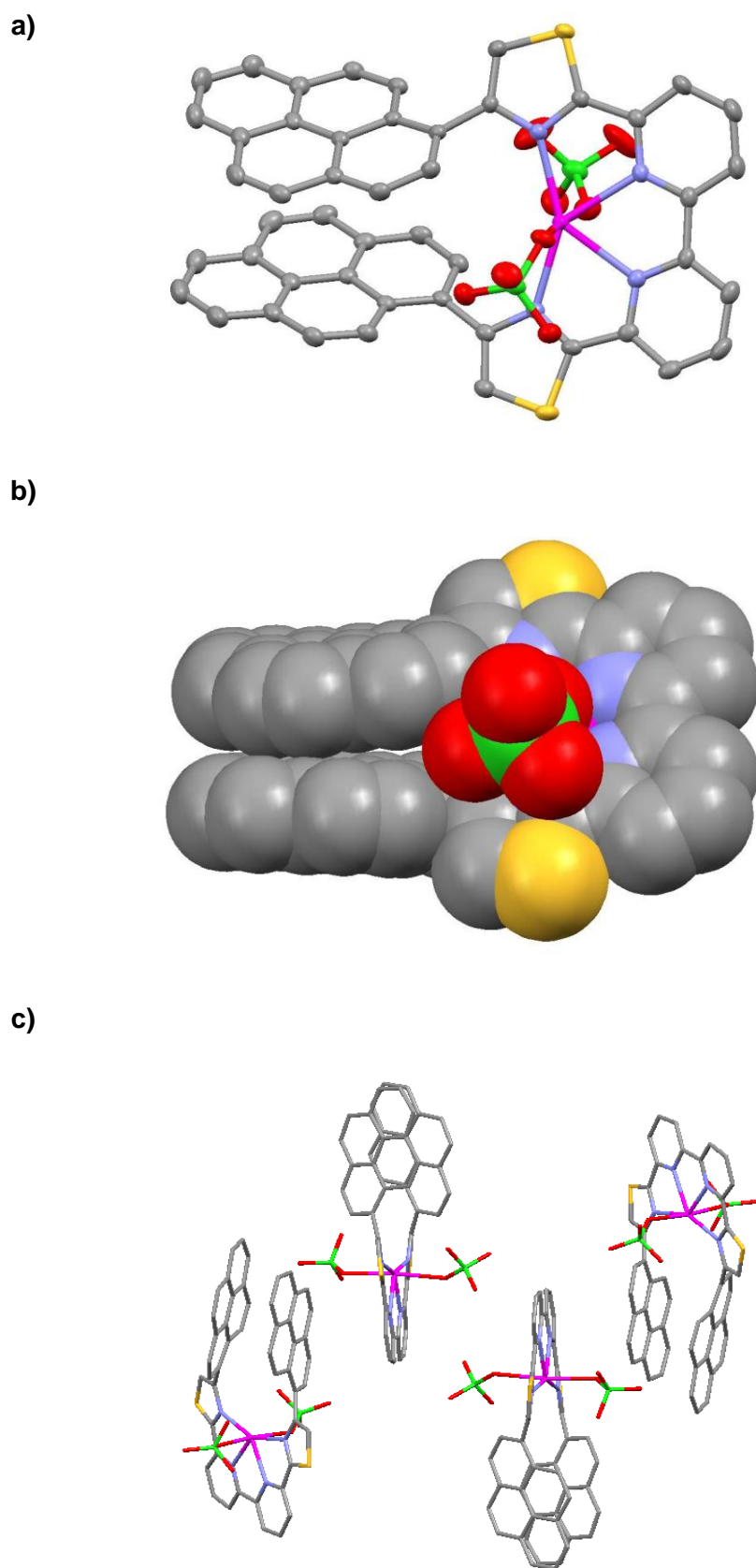
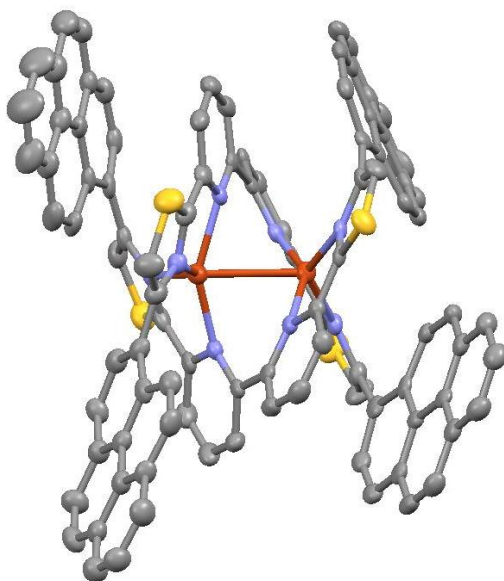


Fig. 2 The single crystal structure of $\{[Cd(L^2)](ClO_4)_2\}$: (a) as a displacement ellipsoid plot drawn at the 50% probability level; (b) as a space-filling model; (c) showing the molecular packing in the unit cell (solvent molecules omitted for clarity)

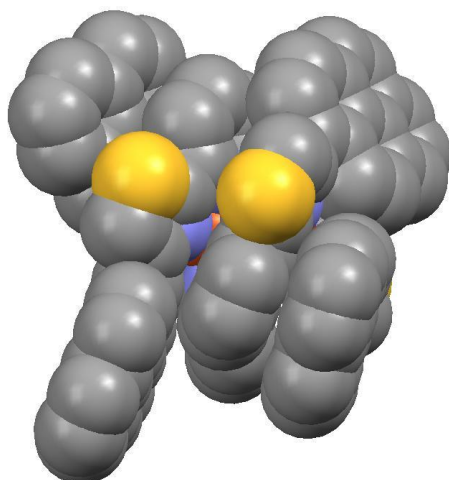
Reaction of L^2 with $Cu(MeCN)_4PF_6$

Reaction of L^2 with one equivalent of $Cu(MeCN)_4PF_6$ in $MeNO_2$ in the presence of excess Et_4NClO_4 afforded a red solution from which red crystals were obtained upon slow diffusion of ethyl acetate. Solution state analyses indicated formation of the dinuclear double helicate species $[Cu_2(L^2)_2]^{2+}$; an ion was observed in the ESI-mass spectrum at m/z 1717.2 corresponding to $\{[Cu_2(L^2)_2](PF_6)\}^+$. The 1H NMR spectrum (CD_3CN) was also consistent with formation of the $[Cu_2(L^2)_2]^{2+}$ complex; 13 aromatic signals were present indicating that a symmetrical species is formed. Some of these signals showed line broadening which can be attributed to hindered rotation of the pyrene groups in the double helicate assembly; heating the sample to 343 K failed to improve the peak shapes. The formation of the dinuclear double helicate was confirmed by single crystal X-ray analysis which showed that the ligand partitions into two bidentate *N*-donor domains with each copper ion coordinated by two of these bidentate domains, one from each ligand (Fig. 3a,b). The Cu(I) centre adopts a distorted tetrahedral geometry with Cu–N distances ranging from 2.050(4) to 2.132(4) Å. Each of the pyrene units lies at the end of a ligand strand; the intramolecular pyrene–pyrene separation is quite large with intrastrand centroid...centroid distances of 8.080 and 8.315 Å (*cf.* 3.783 Å in the $[Cd(L^2)]^{2+}$ species); the interstrand centroid...centroid distances are 8.669 and 9.241 Å. Examination of the intermolecular packing shows that the pyrene units align in an edge-to-face arrangement in an analogous manner to $[Cu_2(L^1)_2]^{2+}$ with the shortest centroid...centroid distance being 6.077 Å (Fig. 3c).

a)



b)



c)

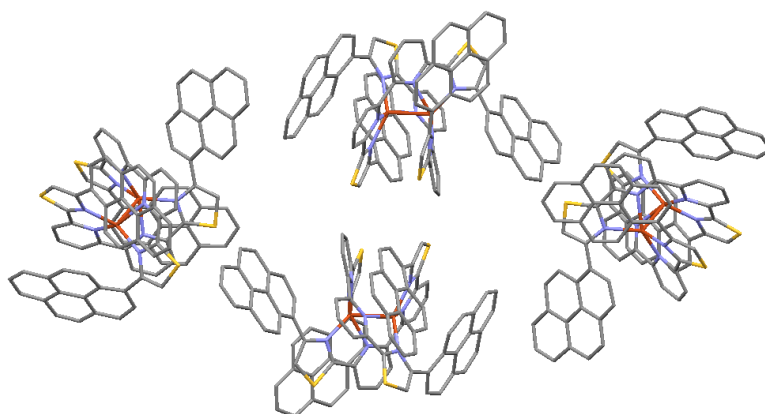


Fig. 3 The single crystal structure of [Cu₂L₂]²⁺: (a) as a displacement ellipsoid plot drawn at the 50% probability level; (b) as a space-filling model; (c) showing the molecular packing in the unit cell (counter ions and solvent molecules omitted for clarity)

Photophysical measurements

The steady state spectrum of the dilute free ligand L^1 (10^{-6} M) was dominated by a broad emission band at 462 nm (with a corresponding lifetime of 1.1 ns), which is characteristic of an excimer-based fluorescent emission: upon further sequential dilutions of the free ligand evidence of the monomeric pyrene emission appeared as vibronically structured features at 370–440 nm (Fig. 4).

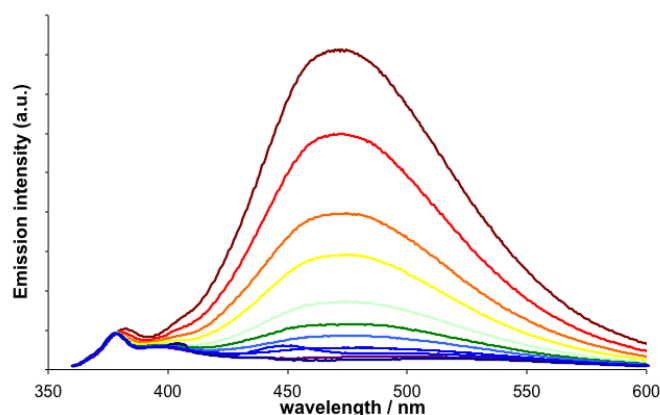


Fig. 4 Emission spectra (MeCN; $\lambda_{ex} = 340$ nm) for L^1 with decreasing concentration (2.1×10^{-6} M to 2.1×10^{-9} M)

Addition of either Cd^{2+} or Cu^+ to 2.1×10^{-6} M L^1 resulted in a decrease in intensity of the excimer band and the formation of new features at higher energy (360–460 nm) attributed to monomeric pyrene fluorescence. For the complexes this higher energy fluorescence was associated with lifetimes of 4.1–6.9 ns and therefore easily distinguished from the shorter-lived excimer emission of the corresponding free ligand (Fig. 5).

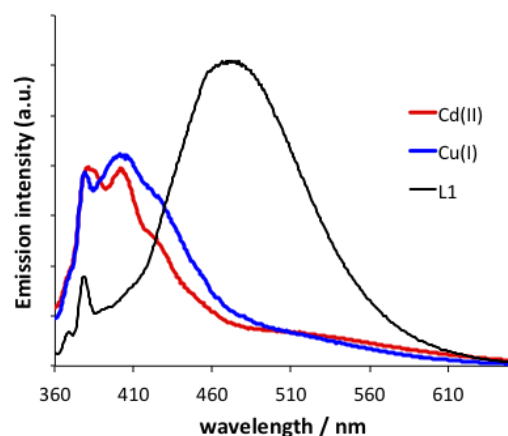


Fig. 5 Comparison of the emission spectra (2.1×10^{-6} M MeCN; $\lambda_{ex} = 340$ nm) of L^1 , $[Cd(L^1)]^{2+}$ and $[Cu_2(L^1)_2]^{2+}$

In contrast to L^1 , the steady state spectrum of bis-pyrenyl L^2 (1.7×10^{-6} M) was dominated by typical monomeric pyrene emission, with classical vibronic features prominently displayed between 360–450 nm, and a corresponding lifetime of 5.5 ns. Mixing of this ligand at 1.7×10^{-6} M with Cu^+

gave an emission spectrum almost superimposable with that of the free ligand, but with a slight increase in emission intensity and a notable reduction in the resolution of the vibronic structure. However, reaction with Cd^{2+} resulted in a significant quenching of the overall emission intensity and the spectrum showed an additional weakly intense band at ca. 540 nm, which is tentatively attributed to excimeric emission (Fig. 6).

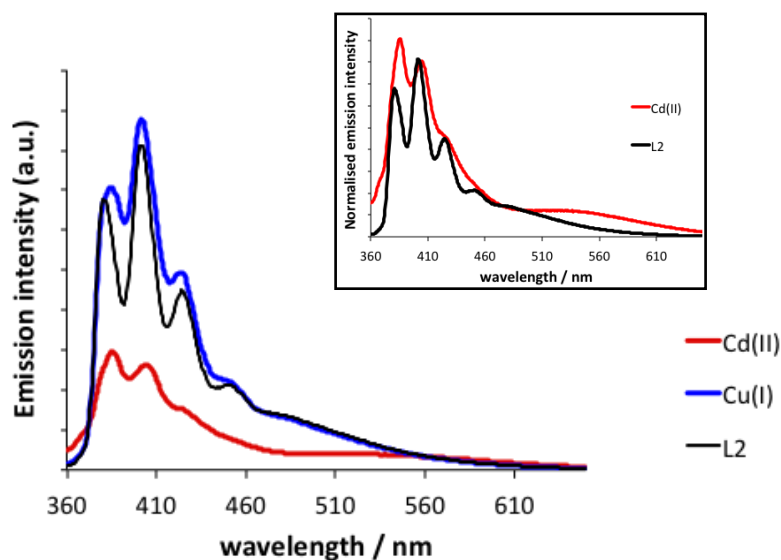


Fig. 6 Comparison of the emission spectra (1.7×10^{-6} M MeCN; $\lambda_{\text{ex}} = 340$ nm) of L^2 , $[\text{Cd}(\text{L}^2)]^{2+}$ and $[\text{Cu}_2(\text{L}^2)_2]^{2+}$. Inset: Comparison of the normalized (400 nm) emission spectra of L^2 and $[\text{Cd}(\text{L}^2)]^{2+}$

The spectra for $[\text{Cd}(\text{L}^1)]^{2+}$ and $[\text{Cu}_2(\text{L}^1)_2]^{2+}$ both reveal monomer pyrene emission, with no emission attributable to excimer formation: this corroborates the solid state structures since there are no proximate pyrene units. The emission spectra of both $[\text{Cd}(\text{L}^1)]^{2+}$ and $[\text{Cu}_2(\text{L}^1)_2]^{2+}$ are remarkably similar indicating that the metal ions (which are of different oxidation states) have markedly little effect on the emission profile. However, comparison of the complexes $[\text{Cd}(\text{L}^2)]^{2+}$ and $[\text{Cu}_2(\text{L}^2)_2]^{2+}$ shows that these two complexes give different emission profiles. Upon reaction of L^2 with Cu^+ little change in the emission spectrum is observed (Fig. 6), whereas for $[\text{Cd}(\text{L}^2)]^{2+}$ a general quenching is observed together with a new, weak emission at 540 nm (Fig. 6, inset). The difference in the emissive properties of these two species due to the different metal ions and their respective oxidation states can be discounted due to the similarity of the photophysical properties of $[\text{Cd}(\text{L}^1)]^{2+}$ and $[\text{Cu}_2(\text{L}^1)_2]^{2+}$. The differences must arise from the proximity of the appended pyrene units: in the copper-containing species the two pyrene units are distant (and the spectra show monomeric emission), whereas for the cadmium complex the two pyrene units are in close proximity giving rise to a general quenching together with a new, but weak emission at 540 nm both consistent with excimer formation. Furthermore, the difference in emission behaviour cannot be attributed to the intermolecular interactions as both the copper-containing species show the shortest pyrene–

pyrene interactions (relatively) at 6.591 and 6.077 Å and both of these complexes show monomer emission (and hence no energy transmission between the chromophoric units). The intermolecular distances between the pyrene units are much longer in the cadmium complex (9.915 Å) which displays excimer emission and due to the close intramolecular proximity of the pyrene units (3.783 Å) it seems highly likely that it is this interaction that gives rise to the energy transfer. Although these are solid state measurements, the luminescence behaviour observed supports the inference that the molecules do not interact significantly in solution and that any excimer emission arises as a consequence of intramolecular associations.

These solution state spectroscopic results suggest that inclusion of pyrene units within a ligand strand can help ascertain the self-assembled species in solution through monitoring of monomer *versus* excimer type emission from the fluorescent pyrene units.

Conclusion

Fluorescent pyrene units can be successfully incorporated into multidentate ligands targeting helical structures. The inclusion of a pyrene unit within a ligand strand can be a useful probe into the resultant self-assembled species due to the environmentally sensitive fluorescent properties of the pyrene chromophore. Although subtle, the differences in the emission spectra for $[\text{Cd}(\text{L}^2)]^{2+}$ and $[\text{Cu}_2(\text{L}^2)_2]^{2+}$ are consistent with the structures observed in the solid state.

Experimental

General

All photophysical data were obtained on a Jobin Yvon-Horiba Fluorolog spectrometer fitted with a JY TBX picosecond photodetection module. Lifetimes were obtained using the provided deconvolution software DAS6. Electrospray ionisation mass spectra were recorded from 10^{-3} M solutions on a Bruker MicrOTOF-q instrument. Assignments of ions from the mass spectra of the complexes were confirmed by comparison of the measured and calculated isotope patterns for each species. NMR spectra were recorded on a Bruker DPX400 MHz spectrometer. The ligands and complexes were, in some cases, poorly soluble leading to broad, unresolved peaks which were frequently coincident with other signals.

Synthesis of ligands

Synthesis of the potentially tetradentate ligand L¹. 2,2':6'2''-Terpyridine-6-thioamide (0.05 g, 0.17 mmol) and 1-(bromoacetyl)pyrene (0.129 g, 0.40 mmol) were placed into a 100 mL round bottomed flask. Ethanol (50 mL) was added and the reaction was heated under reflux for 12 h. The product was filtered under vacuum then washed with ethanol followed by diethyl ether. The product was then suspended in ammonia (10 mL) for 20 h, filtered under vacuum and washed with water, ethanol and diethyl ether.

$^1\text{H NMR}$ = [400 MHz, d_6 -DMSO] δ 8.82 (m, 3H, overlap), 8.75 (d, J = 8.2, 1H, py), 8.67 (d, J = 7.6, 1H, py), 8.59 (d, J = 7.9, 1H, py), 8.47 (m, 2H, overlap) 8.41 (m, 4H, overlap), 8.31 (m, 5H, overlap), 8.18 (t, J = 7.6, 1H, py), 8.10 (dt, J = 7.6/1.6, 1H, py), 7.58 (dt, J = 6.1/1.8Hz, 1H, py).

ESI-MS found m/z = 517.1 $[\text{M}+\text{H}]^+$, HR-ESI-MS found 517.1475, $\text{C}_{34}\text{H}_{21}\text{N}_4\text{S}_1$ requires 517.1481.

Synthesis of the potentially tetradentate ligand L^2 . 1-(Bromoacetyl)pyrene (0.129 g, 0.40 mmol) was placed in a 100 mL round bottomed flask. 2,2'-Bipyridine-6,6'-dithioamide (0.05 g, 0.18 mmol) and ethanol (50 mL) were added to the flask and the reaction was heated under reflux for 12 h. The solution was filtered under vacuum then washed with ethanol followed by diethyl ether. The dried precipitate was suspended in ammonia (10 mL) for 20 h then filtered under vacuum. The product was washed with water, ethanol and diethyl ether.

ESI-MS found m/z = 723.1 $[\text{M}+\text{H}]^+$, HR-ESI-MS found 723.1675, $\text{C}_{48}\text{H}_{27}\text{N}_4\text{S}_2$ requires 723.1672.

It was not possible to assign the ^1H NMR spectrum (recorded in d_6 -DMSO) as the ligand was very sparingly soluble; the spectrum showed a number of aromatic signals but these were weak and poorly resolved.

Crystallographic data

Single crystal X-ray diffraction data were collected either at 100(2) or 150(2) K on a Bruker Apex Duo diffractometer equipped with a graphite monochromated $\text{Mo}(\text{K}\alpha)$ radiation source and a cold stream of N_2 gas.

Crystal data for $\{[\text{Cu}_2\text{L}^1_2](\text{PF}_6)_2\}$ ($\text{C}_{68}\text{H}_{40}\text{Cu}_2\text{N}_8\text{S}_2\cdot 2\text{PF}_6$). $M = 4348.64$; Orthorhombic, $Iba2$, $a = 45.237(2)$, $b = 18.6322(10)$, $c = 23.8739(13)$ Å, $V = 20122.5(2)$ Å³, $Z = 4$; $\rho_{\text{calc}} = 1.435$ Mg m⁻³, $F(000) = 8776$; dimensions 0.35 x 0.12 x 0.10 mm; $\mu(\text{Mo-K}\alpha) = 0.71073$ mm⁻¹, $T = 150$ K. A total of 31846 reflections were measured in the range $2.08 \leq \theta \leq 23.31^\circ$ (hkl range indices: $-48 \leq h \leq 50$, $-20 \leq k \leq 20$, $-21 \leq l \leq 26$), 12922 unique reflections ($R_{\text{int}} = 0.0377$). The structure was refined on F^2 to $R_w = 0.1813$, $R = 0.0660$ (10183 reflections with $I > 2\sigma(I)$) and GOF = 1.015 on F^2 for 1227 refined parameters, 949 restraints. Largest peak and hole 1.057 and -0.617 e Å⁻³. CCDC 845594. The crystals were highly solvated and during inspection they appeared to undergo decomposition giving a poorly diffracting species; despite exhaustive attempts an improved species could not be produced. As a result voids are present within the crystal unit and there is a low ratio of data to parameters. A hexafluorophosphate anion was disordered and was modelled over two sites; the remaining hexafluorophosphate anions showed some disorder and the SHELXTL restraints DFIX, DELU and SIMU were used in the refinement. Some of the carbon atoms also showed disorder and were restrained using the DELU and SIMU instruction. However, the structure does give the overall atom connectivity and supports the finding reported here.

Crystal data for $\{[\text{Cd}(\text{L}^2)](\text{ClO}_4)_2\text{MeNO}_2\}$ ($\text{C}_{48}\text{H}_{26}\text{CdN}_4\text{S}_2\cdot \text{CH}_3\text{NO}_2\cdot 2\text{ClO}_4$). $M = 1095.19$; Monoclinic, $P2_1/c$, $a = 20.2402(8)$, $b = 10.3881(4)$, $c = 20.5791(7)$ Å, $\beta = 101.4650(10)^\circ$, $V = 4240.6(3)$ Å³, $Z = 4$; $\rho_{\text{calc}} = 1.715$ Mg m⁻³, $F(000) = 2208$; dimensions 0.40 x 0.35 x 0.07 mm; $\mu(\text{Mo-}$

$K\alpha$) = 0.71073 mm⁻¹, $T = 101$ K. A total of 38944 reflections were measured in the range $2.02 \leq \theta \leq 27.88^\circ$ (hkl range indices: $-26 \leq h \leq 26$, $-13 \leq k \leq 13$, $-27 \leq l \leq 26$), 10120 unique reflections ($R_{\text{int}} = 0.0483$). The structure was refined on F^2 to $R_w = 0.0800$, $R = 0.0330$ (8049 reflections with $I > 2\sigma(I)$) and GOF = 0.950 on F^2 for 623 refined parameters, 0 restraints. Largest peak and hole 0.637 and -0.653 e Å⁻³. CCDC 845595.

Crystal data for {[Cu₂L₂](ClO₄)₂MeNO₂EtOAc} (C₉₆H₅₂Cu₂N₈S₄·C₄H₈O₂·CH₃NO₂·2ClO₄). $M = 1920.82$; Monoclinic, $P2_1/n$, $a = 15.462(2)$, $b = 33.213(5)$, $c = 16.066(2)$ Å, $\beta = 98.734(2)^\circ$, $V = 8155.0(2)$ Å³, $Z = 4$; $\rho_{\text{calc}} = 1.564$ Mg m⁻³, $F(000) = 3936$; dimensions 0.500 x 0.250 x 0.050 mm; $\mu(\text{Mo-K}\alpha) = 0.71073$ mm⁻¹, $T = 150(2)$ K. A total of 63702 reflections were measured in the range $1.77 \leq \theta \leq 26.43^\circ$ (hkl range indices: $-19 \leq h \leq 18$, $-41 \leq k \leq 41$, $-19 \leq l \leq 20$), 16577 unique reflections ($R_{\text{int}} = 0.0692$). The structure was refined on F^2 to $R_w = 0.1498$, $R = 0.0629$ (9947 reflections with $I > 2\sigma(I)$) and GOF = 1.006 on F^2 for 1175 refined parameters, 41 restraints. Largest peak and hole 1.059 and -0.827 e Å⁻³. The ethyl acetate solvent molecule was disordered and was restrained using DELU and SIMU instructions during the refinement. CCDC 845596.

References

1. J.-M. Lehn, *Supramolecular Chemistry*, VCH, Weinheim, 1995; E.C. Constable, in *Comprehensive Supramolecular Chemistry, vol. 9; Polynuclear Transition Metal Helicates*, ed. J.-P. Sauvage, Elsevier, Oxford, 1996; C. Piguet, G. Bernardinelli and G. Hopfgartner, *Chem. Rev.*, 1997, **97**, 2005–2062; M. Albrecht, *Chem. Rev.*, 2001, **101**, 3457–3497; M.J. Hannon and L.J. Childs, *Supramol. Chem.*, 2004, **16**(1), 7–22; T. Krickmann and F.E. Hahn, *Chem. Commun.*, 2007, 1111–1120.
2. D.B. Dell' Amico, F. Calderazzo, M. Curiardi, L. Labella and F. Marchetti, *Inorg. Chem.*, 2004, **43**(17), 5459–5465.
3. E.C. Constable, M.J. Hannon, A. Martin, P.R. Raithby and D.A. Tocher, *Polyhedron*, 1992, **11**, 2967–2971.
4. P. Hammarström, B. Kalman, B.-H. Jonsson and U. Carlsson, *FEBS Lett.*, 1997, **420**, 63–68; M. K. Santra, D. Dasgupta and D. Panda, *Photochem. Photobiol.*, 2006, **82**, 480–486; P. B. Conibear, C.R. Bagshaw, P.G. Fajer, M. Kovacs and A. Malnasi-Csizmadia, *Nat. Struct. Biol.*, 2003, **10**(10), 831–5.
5. A.A. Martí, X. Li, S. Jockusch, Z. Li, B. Raveendra, S. Kalachikov, J.J. Russo, I. Morozova, S.V. Puthanveetil, J. Ju and N.J. Turro, *Nucleic Acids Res.*, 2006, **34**(10), 3161–3168; P.L. Paris, J.M. Langenhan and E.T. Kool, *Nucleic Acids Res.*, 1998, **26**(16), 3789–3793.
6. D. Mansell, N. Rattray, L.L. Etchells, C.H. Schwalbe, A.J. Blake, E.V. Bichenkova, R.A. Bryce, C.J. Barker, A. Díaz, C. Kremer and S. Freeman, *Chem. Commun.*, 2008, 5161–5163.
7. Z. Xu, N.J. Singh, J. Lim, J. Pan, H.N. Kim, S. Park, K.S. Kim and J. Yoon, *J. Am. Chem. Soc.*, 2009, **131**, 15528–15533.

8. L. Zeng, P. Wang, H. Zhang, X. Zhuang, Q. Dai and W. Liu, *Org. Lett.*, 2009, **11**(19), 4294–4297.
9. F. Schmidt, S. Stadlbauer and B. König, *Dalton Trans.*, 2010, **39**, 7250–7261.
10. D.Y. Sasaki and B.E. Padilla, *Chem. Commun.*, 1998, 1581–1582; S. Leroy, T. Soujanya and F. Fages, *Tetrahedron Lett.*, 2001, **42**, 1665–1667; A.C. Benniston, A. Harriman, D.J. Lawrie, A. Mayeux, K. Rafferty and O.D. Russell, *Dalton Trans.*, **2003**, 4762–4769; H.-C. Hung, C.-W. Cheng, I.-T. Ho and W.-S. Chung, *Tetrahedron Lett.*, 2009, **50**, 302–305; T. Moriuchi-Kawakami, Y. Hisada and Y. Shibutani, *Chem. Cent. J.*, 2010, **4**, 7; Y. Yang, X. Gou, J. Blecha and H. Cao, *Tetrahedron Lett.*, 2010, **51**, 3422–3425.
11. S. Kyatskaya, J. R. G. Mascarós, L. Bogani, F. Henrich, M. Kappes, W. Wernsdorfer and M. Ruben, *J. Am. Chem. Soc.*, 2009, **131**, 15143–15151; M. Urdampilleta, S. Klyatskaya, J.-P. Cleuziou, M. Ruben and W. Wernsdorfer, *Nat. Mater.*, 2011, **10**, 502–506.
12. M.T. Indelli, M. Ghirotti, A. Prodi, C. Chiorboli, F. Scandola, N.D. McClenaghan, F. Puntoriero and S. Campagna, *Inorg. Chem.*, 2003, **42**, 5489–5497; A. Sautter, B.K. Kaletas, D.G. Schmid, R. Dobrawa, M. Zimine, G. Jung, I.H.M. van Stokkum, L. De Cola, R.M. Williams and F. Würthner, *J. Am. Chem. Soc.*, 2005, **127**, 6719–6729.
13. J.-X. Jiang, A. Trewin, D. J. Adams and A.I. Cooper, *Chem. Sci.*, 2011, **2**, 1777–1781.
14. C.R. Rice, S. Wörl, J.C. Jeffery, R.L. Paul and M.D. Ward, *Chem. Commun.*, 2000, 1529–1530; C.R. Rice, S. Wörl, J.C. Jeffery, R. L. Paul and M.D. Ward, *J. Chem. Soc., Dalton Trans.*, **2001**, 550–559; C.R. Rice, C.J. Baylies, L.P. Harding, J.C. Jeffery, R.L. Paul and M.D. Ward, *J. Chem. Soc., Dalton Trans.*, **2001**, 3039–3044; C.R. Rice, C.J. Baylies, L.P. Harding, J.C. Jeffery, R.L. Paul and M.D. Ward, *Polyhedron*, 2003, **22**, 755–762.

Notes

^a Dept of Chemical & Biological Sciences, University of Huddersfield, Huddersfield, HD1 3DH, UK. Fax: (+44) 1484 472182; Tel: (+44) 1484 472434; E-mail: l.p.harding@hud.ac.uk

^b School of Chemistry, Main Building, Cardiff University, Museum Avenue, Cardiff, CF10 3AT, UK.